INTERTIDAL FINGER BARS AT EL PUNTAL, BAY OF SANTANDER, SPAIN. A MORPHOLOGICAL MODELLING STUDY.

Roland Garnier[1], Erica Pellón[2], Raúl Medina[3] and Albert Falqués[4]

Abstract

The Bay of Santander is one of the largest inlets in the northern coast of Spain. It is bounded northward by a natural 2.5km-long sand spit: El Puntal. The beaches lying in the southern part are protected from the incoming swells. These beaches exhibit a persistent rhythmic bar system characterized by 15-20 shore-attached bars with an oblique orientation with respect to the shoreline. The mean spacing between two bars is 25m. Preliminary studies have characterized the behavior of these bars by means of video imagery showing that the dynamics is complex and can be governed by various forcing. The objective of this contribution is to further understand the bar dynamics by the use of a morphological numerical model

Key words: intertidal finger bar, estuarine morphodynamics, surf-zone morphodynamics, self-organization.

1. Introduction

The Bay of Santander is one of the largest inlets in the northern coast of Spain. It is bounded northward by a natural 2.5km-long sand spit: El Puntal. While the northern face of El Puntal spit is exposed to the Atlantic Ocean, the beaches lying in the southern part are protected from the incoming swells. These beaches exhibit a persistent rhythmic bar system characterized by 15-20 shore-attached bars with an oblique orientation with respect to the shoreline (Garnier et al., 2012). The mean spacing between two bars is 25m.

By means of video imagery (Medina et al., 2007), Garnier et al. (2012) have characterized the behavior of these bars showing that they migrate slowly (6cm/day) against the ebb-current and that their positions oscillate with a period of 15 days. Preliminary analysis of climate data has shown the complexity in the dynamics of such bar system, showing that the dynamics of these bars can be controlled by the wind, by the wave generated by the wind, by the gradient in sea level due to tide, or by the water discharge of the Miera river that ends at 2 km from the study site.

The objective of this contribution is to further understand the bar dynamics by the use of a morphological numerical model. This will allow us to get insight in the possible formation mechanism and in the main processes governing the bar migration.

[1]Environmental Hydraulics Institute "IH Cantabria", Universidad de Cantabria, c /Isabel Torres nº 15, Santander, 39011, Spain. garnierr@unican.es

[2]Environmental Hydraulics Institute "IH Cantabria", Universidad de Cantabria, c /Isabel Torres nº 15, Santander, 39011, Spain. pellone@unican.es

[3]Environmental Hydraulics Institute "IH Cantabria", Universidad de Cantabria, c /Isabel Torres nº 15, Santander, 39011, Spain. medinar@unican.es

[4]Applied Physics Dept, Universitat Politécnica de Catalunya, C/ Jordi Girona 1-3, Barcelona, 08034, Spain. falques@fa.upc.edu

2. The Intertidal Finger Bar System at El Puntal

2.1. *Study Site*

El Puntal spit is a 2.5km-long sandy spit with a W-E orientation, exposed northward to the Atlantic Ocean and protected southward from the incoming swell. Although the morphology of beaches in the northern face of El Puntal is very well documented (see for instance Losada et al., 1992 and Medellín et al., 2008, 2009, Gutierrez et al., 2011), specific studies on the southern beaches are sparse (Garnier et al., 2012). One particularity of the southern beaches is the presence of elongated (finger) sand bars that appear in the intertidal zone (Figure 1).

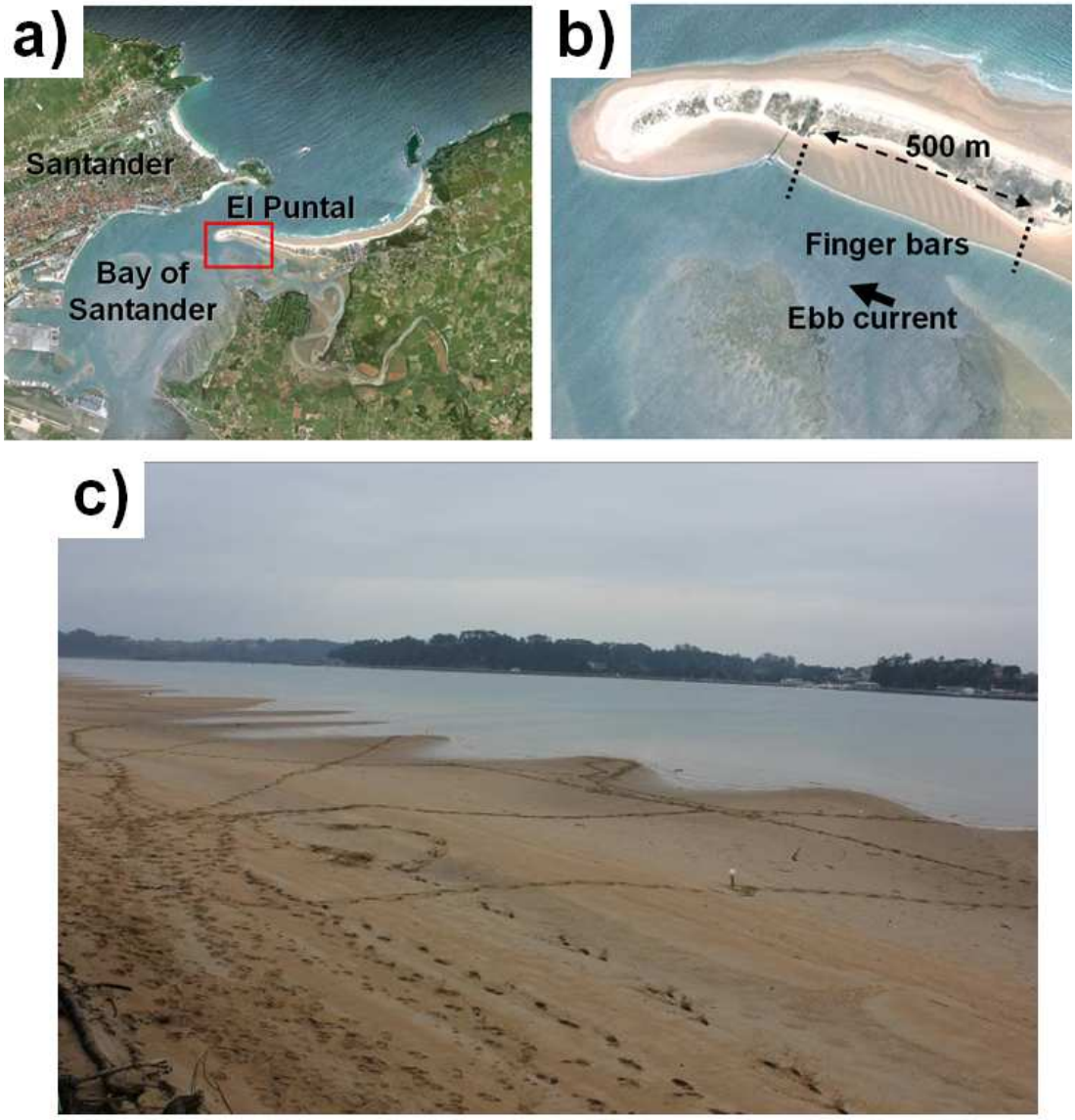

Figure 1. Study site. (a) Localization of the Bay of Santander. (b) Zoom of the intertidal finger bars at El Puntal spit at low tide. Image source: Google Earth imagery © DigitalGlobe and GeoEye. (c) Photo of the bar system at mid-tide, the coastline exhibits a cuspate shape. Adapted from Garnier et al., 2012.

2.2. *Bar Behavior and Possible Forcing*

From 2008, a video monitoring of these bedform has been performed by the recently developed Horus system (www.horusvideo.com, Medina et al., 2007). The Horus video system consists of four video cameras pointing to El Puntal spit, located at 1.5km westward of the bar system. In the study area the video system provides a pixel resolution of 0.5 m in the cross-shore direction and 5 m in the alongshore direction. Daily images from June 2008 to June 2010 have been analyzed to characterize the dynamics of the bar system (Garnier et al., 2012).

Figure 2 show the evolution of Bar 10 (From Garnier et al., 2012). It is characterized by a net positive translation during the 2 year survey, showing that the bar migrates to the east (to the inside of the bay) at a net speed of 6 cm/day for 2 years. Moreover, we observe 'fast' oscillations that can be captured by subtracting the bar position with its 22 day moving average. This fast movement is characterized by velocities higher than +/-10 m/day a 10% of time (negative velocities mean migration to the west). Interestingly, the Fourier analysis of the position signal gives a maximum at 15 days (not shown) that corresponds to the spring tides period. Finally, the slow evolution of the bars obtained with the 22 day moving average shows velocities of up to +/-0.7 m/day.

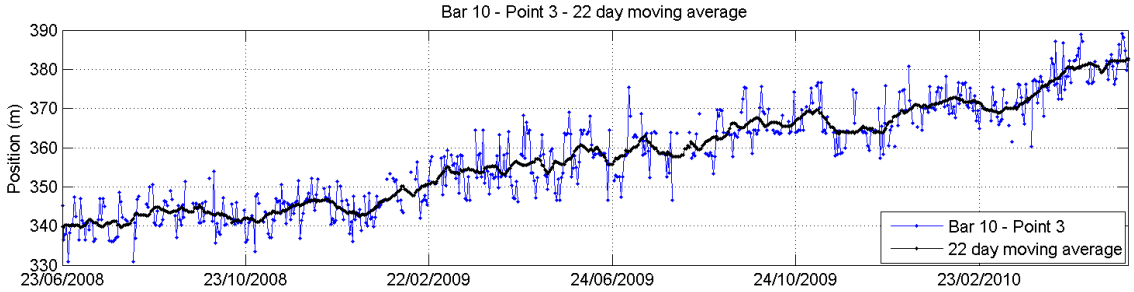

Figure 2. Analysis of the position of Bar 10. Position of Bar 10 (blue line) and its 22 day moving average (black line). Adapted from Garnier et al., 2012.

The period of the fast movement of the bar is 15 days and corresponds to the period of the spring tides. This suggests the effect of the tide in the bar dynamics. However, an analysis of climate data (Garnier et al., 2012) shows that other forcings probably act on the bar dynamics as the slow motion observed (+/- 0.7 m/day) is not related to tidal variations. We indentified other possible forcings that are the wind (blowing predominantly from the west), the waves generated by the wind (maximum fetch is 4km in the SW direction), and also the water discharge of the Miera river that ends at 2 km east of the study site.

However, the correlation between the bar movement and each climate variable, taken as separately is poor, this is probably explained as the dynamics of the bar is due to the combination and to the interaction of the different forcings. Moreover, during the survey period, the bar system never disappear so that there is no information on the formation of the entire system.

3. Numerical Model

The use of a morphological numerical model is needed in order to understand the possible mechanisms that could explain the initial formation of the bar system, and also to understand the observed bar movement by considering the different forcings taken by separately or by combining them.

We use the MORFO55 nonlinear numerical model based on a wave and depth averaged shallow water equation solver with wave driver, sediment transport and bed updating. The governing equations have already been presented by Caballeria et al., 2002; Garnier et al., 2006; 2008 and 2010. It is able to reproduce the formation and the long-term evolution of rhythmic sand bars as free instabilities of alongshore uniform beaches excited by a small perturbation added on the initial topography (Garnier et al., 2006).

The coastline is assumed to be rectilinear and is defined as $x_1 = 0$, $x=x_1$ and $y=x_2$ denoting the cross-shore and the alongshore coordinate, respectively. Sea level variation is assumed to be constant so that the behavior of the finger bar system is analyzed by considering that they are permanently underwater.

3.1. *Hydrodynamics*

The hydrodynamics are governed by the depth and wave averaged mass (1) and momentum (2) conservation equations described by Mei (1989) which read (Garnier et al., 2006):

$$\frac{\partial D}{\partial t} + \frac{\partial}{\partial x_j}(Dv_j) = 0 \tag{1}$$

$$\frac{\partial v_i}{\partial t} + v_j \frac{\partial v_i}{\partial x_j} = -g\frac{\partial z_s}{\partial x_i} - \frac{1}{\rho D}\frac{\partial}{\partial x_j}(S_{ij}^{'} - S_{ij}^{''}) + \frac{\tau_{b\,i}}{\rho D} \quad , \quad i = 1,2 \tag{2}$$

where $D(x_1, x_2,t)$ is the total depth, $\mathbf{v}(x_1, x_2,t) = (v_1, v_2)$ is the depth averaged current vector, $z_s(x_1, x_2,t)$ is the mean sea level, g is the gravity acceleration, ρ is the water density, S' is the turbulent Reynolds stress tensor, S'' is the wave radiation stress tensor and $\boldsymbol{\tau_b}$ is the bed shear stress vector.

Wave transformation from the offshore boundary is performed as follows. First, the wave energy density equation (3) including wave-current interaction and irregular waves is considered:

$$\frac{\partial E}{\partial t} + \frac{\partial}{\partial x_j}\left((v_j + c_{g\,j})E\right) + S_{ij}^{'}\frac{\partial v_j}{\partial x_i} = -D \tag{3}$$

where $E(x_1, x_2,t)$ is the energy density defined as $E=1/8\rho g H_{rms}^2$, H_{rms} is the root mean square average of the wave height, $\mathbf{c_g}$ is the group velocity vector of the waves and D the dissipation rate due to wave breaking and bottom friction. Second, the wave vector $\mathbf{k}(x_1, x_2,t)$ is given by using the dispersion relation to compute its modulus k (4) and by the Snell law to have the wave angle θ (5).

$$\sigma^2 = gk\tanh kD \tag{4}$$

$$k.\sin\theta = cte \tag{5}$$

where $\sigma = 2\pi/T$ is supposed to be constant, T is the wave period and θ is defined as the angle between the wave rays and the x_1 axis.

Moreover, forcing due to wind has been included by adding wind stress to the equation (2), as well as forcing due to gradients in sea level due to tide. The tidal forcing can be time dependent, or can be set as constant in order to simulate the residual tidal current only.

The influence of the three forcings can be analyzed by connecting or disconnecting each of them: (1) the wave forcing ($E\neq0$, or $E=0$), (2) the wind and (3) the tide.

Notice that the wave are generated by the local wind (maximum fetch of 4km) as the study site is protected from the swell, thus, E is function of the wind direction and intensity. However, it can be useful to analyze the two forcing by separately in order to study the importance of the waves (and the fetch distance) in the behavior of the bar system.

3.2. *Morphodynamics*

The evolution of the mean bed level $z_b(x_1, x_2,t)$, related with D and z_s by $D=z_s-z_b$, is given by the sediment conservation equation (6):

$$\frac{\partial z_b}{\partial t} + \frac{1}{1-p}\frac{\partial q_j}{\partial x_j} = 0, \tag{6}$$

where **q** is the horizontal sediment flux vector, and p=0.4 is the bed porosity. The sediment flux (7) is based on the total load formula of Soulsby and Van Rijn (Soulsby, 1997) (see details in Garnier et al., 2008). It reads:

$$\vec{q} = \alpha(\vec{v} - \gamma u_b \nabla h), \tag{7}$$

where h is the bottom perturbation with respect to the equilibrium topography ($h=z_b-z_b^0$, where z_b^0 is the initial non-perturbed bed level). u_b is the wave orbital velocity, γ is the bedslope parameter and α is the stirring factor (in m^3/m^2). Two kind of stirring factors can be chosen: (I) first $\alpha=\alpha_{SVR}$, where α is obtained from the Soulsby and Van Rijn formula (SVR, Soulsby 1997), (II) second α is set as constant (see Garnier et al., 2006):

$$\begin{cases} \alpha = \alpha_{\text{SVR}} \\ \alpha = CONSTANT \end{cases}. \tag{8}$$

For the SVR formula, the stirring function is set as:

$$\alpha_{\text{SVR}} = \begin{matrix} A_S (u_S - u_c)^{2.4} \text{ if } u_S > u_c \\ 0 \text{ otherwise} \end{matrix}, \tag{9}$$

according to Soulsby, 1997, where A_S and u_c depend essentially on the sediment characteristics and the water depth (Soulsby, 1997). The stirring velocity u_S reads:

$$u_S = \left(|\vec{v}|^2 + \frac{0.018}{c_D} u_b^2 \right)^{1/2}, \tag{10}$$

c_D being the morphodynamical drag coefficient (Soulsby, 1997).

4. Experiments and Results

4.1. *Experiments*

4.1.1. *Self-organization*

The first kinds of experiments are dedicated to the study of the morphodynamical evolution of an initially alongshore uniform planar beach. Similar experimental setup as Garnier et al. (2006) is used. The initial topography is based on a planar beach profile that is representative of the intertidal zone of the study site. The characteristics have been obtained by mean of the video imagery. If the beach profile is denoted z_b^0, the bed level can be written at the initial time as:

$$z_b(x, y, t=0) = z_b^0(x) + h(x, y, t=0). \tag{11}$$

The initial perturbation h(x,y,t=0) is a small random perturbation. Experiments have been done on the domain defined by: $0 \le x \le L_x = 150$m and $0 \le y \le L_y = 300$m. The grid spacing is given by $\Delta x = 1.5$m and $\Delta y = 3$m. The hydrodynamical time step is defined by the CFL conditions (Garnier et al., 2006). The

morphodynamical processes have been artificially accelerated by a factor 90 (see Garnier et al., 2006).

Test of the three different forcings (wind, wave, tide) will be performed, for different sediment transport formulas (8). First of all, these forcings will be taken as separately; then, the combination of the forcings will be studied. Particularly, we will analyze the combined effect of the wind and of the waves, as they are coupled, and we will add the effect of the tide.

4.1.2. *Migration of the finger bars*

The second kinds of experiments are dedicated to the study of the migration of the finger bars. As the formation processes are hard to identify mainly because the bar system persisted during the survey period. Thus, although the formation of one bar has been identified, the initial formation of the entire system that is assumed to be due to self-organization processes cannot be compared with the field. In other words, the comparison with the field can be performed on the finite amplitude dynamics of the bar system only, and, essentially, on the migration of the finger bars.

To this end, the morphological evolution of pre-existing finger bars will be studied with the morphological numerical model. Initial bathymetry will be set in the same way as Garnier et al., 2010b.

4.2. *Preliminary Results and Further Works*

Figure 3 shows results of the numerical model by considering the forcing due to tide (Figure 3b), wind (Figure 3c) and wind-waves (Figure 3d), by separately. The sediment transport (Equation (8)) as been set such as the stirring factor is constant. We see that all of them can lead to the formation of finger bars with a spacing similar to the one observed. However, none of these specific experiments leads to the observed orientation and to the observed migration direction. For instance, the orientation predicted from wind forcing is opposite to the real orientation (Figure 3c), but the migration direction is correct (toward the east). These discrepancies can be explained because the formation mechanism is due to a combined effect of different forcings, but also because the idealized transport formula used here is not realistic.

Further research is underway and will be presented at the conference. This consists of (1) testing the transport formula of Soulsby and Van Rijn (Equation 9), (2) testing the combining effect of the different forcings and (3) analyzing the finite amplitude behavior of the bar system by starting the simulation from pre-existing (yet formed) features.

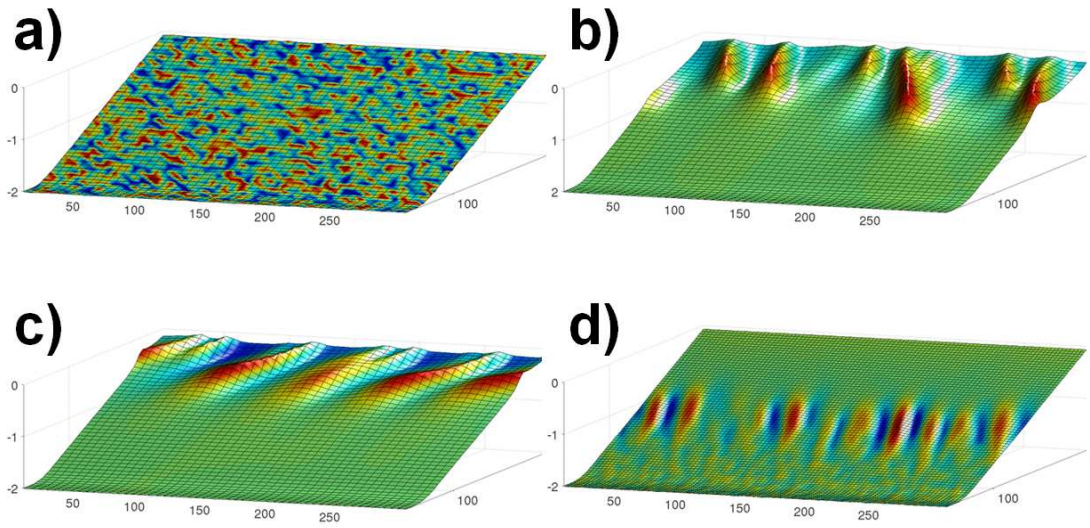

Figure 3. Three-dimensional view of the bed level. The colors represent the bed-level perturbations with respect to the mean profile (shoals are in red, troughs are in blue). (a) Initial bathymetry where random bed-level perturbations have been added. (b) Tidal forcing. (c) Wind forcing. (d) Wind-wave forcing. The experiments are performed by using a constant sediment stirring (Equation 8).

5. Conclusions

Preliminary studies have characterized the behavior of the transverse finger bars at El Puntal spit by means of video imagery. They showed that the dynamics is complex and can be governed by various forcing such as the wind, the wave generated by the wind (maximum fetch: 4km), the gradient in sea level due to tide, or the water discharge of the Miera river that ends at 2 km east of the study site. During the two year survey (2008-2010) there was no information on the formation of the bar system as the bar system was always present. However, the finite amplitude behavior (the migration) of these bars could be characterized.

The results of the morphological nonlinear numerical model MORFO55 have shown that most of these forcing, taken as separately, can generate bars with a spacing similar to the one observed, however, the orientation and the migration is not correctly reproduced. This suggests that the mechanisms of formation are a due to a combined effect of these forcings, or, that the sediment transport formula is not appropriate.

Further research is underway and will be presented at the conference. It consists of testing the other transport formula, testing the combined effect of the different forcings, and analyzing the finite amplitude behavior of the bar system by starting the simulations from pre-existing bedforms.

Acknowledgements

RG acknowledges funding from the Spanish government through the program “Juan de la Cierva”. This research is part of the ANIMO (BIA2012-36822) and IMNOBE (CTM2009-11892) projects which are funded by the Spanish government. The authors thank Puertos del Estado (Spanish Government) for providing tide-gauge data.

References

Caballeria, M., Coco G., Falqués A. and Huntley, D.A., 2002. Self-organization mechanisms for the formation of nearshore crescentic and transverse sand bars. J. Fluid Mech., 465, 379-410.

Garnier, R., Calvete, D., Falqués, A., and Caballeria, M. 2006. Generation and nonlinear evolution of shore-oblique/transverse sand bars. *J. Fluid Mech*., 567: 327-360.

Garnier, R., Calvete, D., Falqués, A. and Dodd, N., 2008. Modelling the formation and the long-term behaviour of rip channel systems from the deformation of a longshore bar. *J. Geophys. Res.*, 113(C07053).

Garnier, R., Dodd, N., Falqués, A. and Calvete, D., 2010. Mechanisms controlling crescentic bar amplitude. *J. Geophys. Res.*, 115: F02007, doi:10.1029/2009JF001407

Garnier, R., Ortega-Sanchez, M., Losada, M.A., Falqués, A., Dodd, N. 2010b. Beach cusps and inner surf zone processes: growth or destruction? A case study of Trafalgar Beach (Cádiz, Spain). *Scientia Marina*, 74(3): 539-553.

Garnier, R., Medina, R., Pellón, E., Falqués, A. and Turki, I. 2012. Intertidal finger bars at El Puntal spit, Bay of Santander, Spain. *In: Coastal Engineering 2012.*

Gutiérrez, O. Q., González, M., Medina, R. 2011. A methodology to study beach morphodynamics based on self-organizing maps and digital images. In. Coastal Sediment, 2011.

Losada, M.A., Medina, R., Vidal, C. and Losada, I.J. 1992. Temporal and spatial cross-shore istributions of sediment at "El Puntal" spit, Santander, Spain. In: Coastal Engineering 1992, 251-2264.

Medellín, G., Medina R., Falqués A. and González M. 2008. Coastline sand waves on a low-energy each at ‘‘El Puntal’’ spit, Spain. Mar. Geol., 250: 143-156.

Medellín, G., Falqués A., Medina R. and González M. 2009. Coastline sand waves on a low-energy each at El Puntal spit, Spain: Linear stability analysis. J. Geophys. Res., 114, C03022, oi:10.1029/2007JC004426.

Medina, R., Marino-Tapia, I., Osorio, A.1, Davidson, M. and Martin F.L. 2007. Management of dynamic navigational channels using video techniques. *Coastal Engineering*, 54, 6-7: 523-537.

Mei, C. C., 1989. *The Applied Dynamics of Ocean Surface Waves, Advanced Series on Ocean Engineering, vol. 1*, World Scientic, Singapore.

Soulsby, R. L., 1997. *Dynamics of Marine Sands*, Thomas Telford, London, U.K.